Using Multiple MFL Magnetizations for Reliable Corrosion Assessment at Scale

Jed Ludlow, Adrian Belanger, Ron Lundstrom, Miguel Maldonado
T.D. Williamson

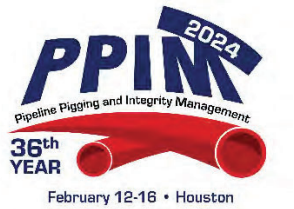

Pipeline Pigging and Integrity Management Conference

February 12-16, 2024

Organized by
Clarion Technical Conferences

https://doi.org/10.52202/072781-0036

https://doi.org/10.52202/072781-0036

Abstract

Reliable assessment of pipeline corrosion remains an important concern for pipeline operators, especially when the corrosion presents itself in complex patterns and in large quantities. We present an approach to this problem using magnetic flux leakage inline inspection employing multiple magnetization directions simultaneously. The approach is accomplished in production data analysis and scales to large quantities of corrosion anomalies.

An axial magnetic flux leakage data set and a spiral magnetic flux leakage data set are gathered simultaneously during the same inline inspection run, and the signals from both data sets are also analyzed simultaneously. Detection, identification, and sizing of metal loss anomalies can be accomplished using one or the other magnetization direction and even a combination of both magnetization directions where appropriate. After sizing, metal loss clusters can be formed from applying interaction rules to combinations of the metal loss anomalies regardless of the data set from which they originate. This facilitates reliable failure pressure estimation using effective area methods even for narrow axial corrosion morphologies that would not be well addressed by conventional axial MFL alone and for other complex corrosion patterns. Application examples demonstrate that comparisons of failure pressures estimated from inline inspection data are in close agreement with those calculated using data from non-destructive evaluation in the ditch.

Introduction

The application of magnetic flux leakage (MFL) techniques by in-line inspection (ILI) for the detection, identification, sizing, and failure pressure assessment of metal loss due to pipeline corrosion remains a critical part of integrity management programs. Technology innovations in the ILI space have resulted in steady performance gains over time. Assessment methods for estimating the failure pressure of corroded pipe have also continued to advance in both sophistication and accuracy. In this paper, we present an additional advancement to the MFL technique, employing multiple MFL magnetization directions simultaneously in conjunction with the effective area method (EAM) for failure pressure assessment. The approach is accomplished in production ILI operations and scales to large quantities of corrosion anomalies.

Background

MFL is a non-destructive technique that has been used to inspect liquid and gas pipelines since the 1960s [1]. This method relies on the magnetic properties of ferrous materials and their specific behavior in response to a strong applied magnetic field. In the case of a pipeline, the field is generated by a magnetizing body on an ILI tool inside the pipe. Any metal loss such as that associated with corrosion will cause the applied flux to "leak" from the pipeline steel into the air just outside the pipe wall. The magnetic flux from a corrosion anomaly, either on the inside or the outside of the pipe, can be measured by magnetic sensors on the ILI tool.

Magnetization Directions

The magnitude and characteristics of the flux signal from metal loss are highly dependent on the direction of the applied magnetizing field. Because of the axisymmetric nature of tubular pipe, the easiest way to design a magnetizer that can provide a uniformly homogenous field is to apply it axially as shown in Figure 1. The short coming of only magnetizing in the axial direction is that metal loss

https://doi.org/10.52202/072781-0036

anomalies that are narrow in the pipe's circumferential direction do not generate much MFL response. In the cases of very narrow axial slotting or axial planar anomalies, the response may be so small as to be practically indistinguishable from the natural background magnetic noise in clean pipeline steel.

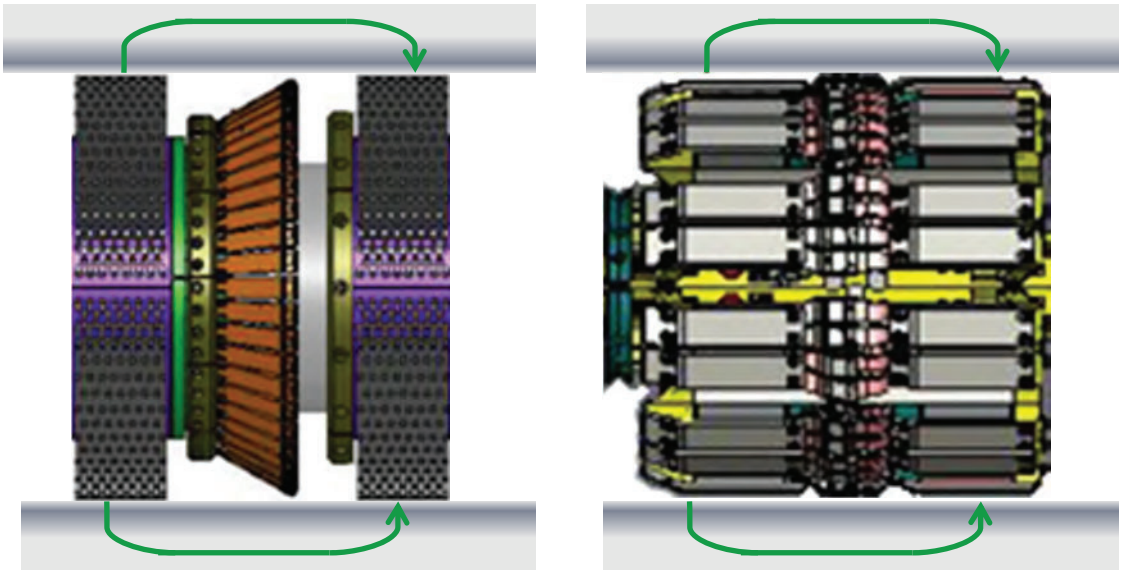

(a) Solid body magnetizer with brushes

(b) Magnetizer with independent articulating magnets

Figure 1. Examples of axial magnetizers applying a magnetic field in the direction of the pipe long axis.

The MFL responses of a groove-like anomaly with large aspect ratio to different angles of applied magnetization are shown in Figure 2. Assume that the long axis of the anomaly is oriented parallel to the long axis of the pipe. If an axial magnetizer is applied, the magnetization direction would be parallel to the long axis of the anomaly. The MFL signal (upper-right color map in Figure 2), while detectable, is small and only somewhat indicative of the underlying anomaly geometry. By magnetizing circumferentially [2] [3], the applied field is perpendicular to the long axis, generating the maximum amount of MFL signal (center-right color map in Figure 2). However, it is also possible to obtain a significant MFL signal response by magnetizing at an angle that is neither parallel nor perpendicular to the long axis. The bottom-right color map plot in Figure 2 shows an MFL response obtained by magnetizing at 45 degrees to the long axis. Its amplitude is only slightly reduced from the full circumferential response [4].

https://doi.org/10.52202/072781-0036

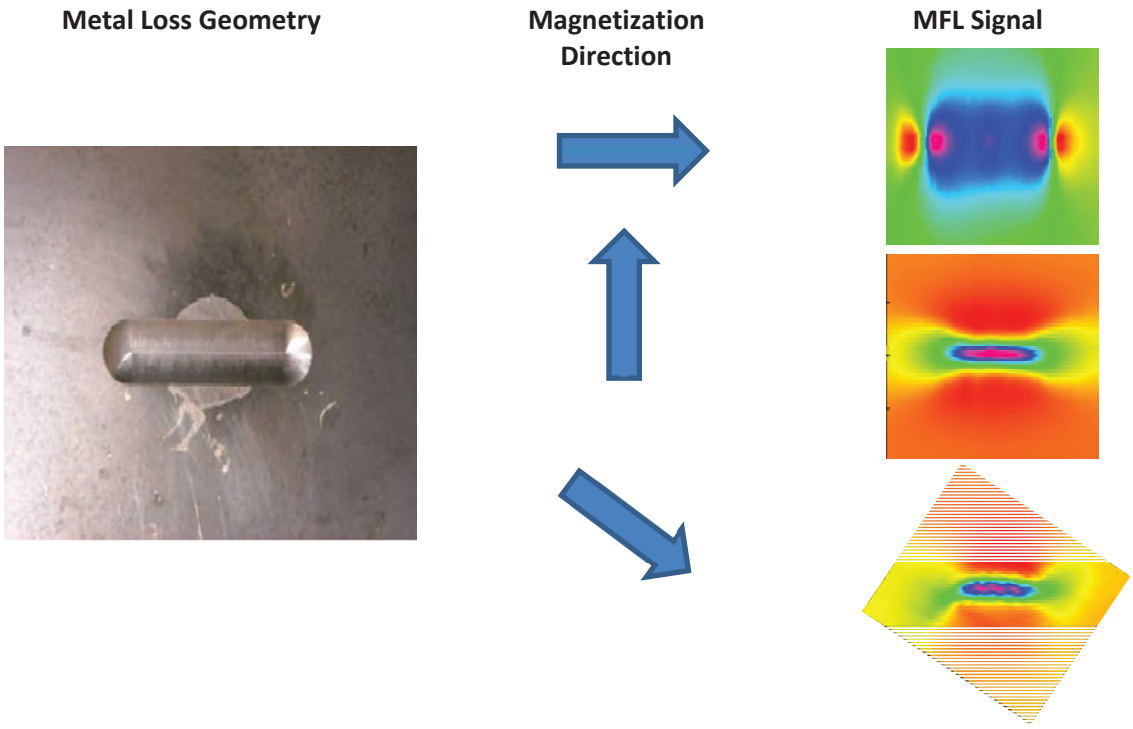

Figure 2. Magnetization direction influences the MFL signal from a metal loss anomaly.

Metal Loss Sizing Approaches

Early MFL implementations focused on qualitative prioritization of anomalies based on signal strength. Approaches to quantitatively estimating the size of anomalies from axial MFL data are described as early as the late 1990s [5, 6]. More recently, in relation to the problem of sizing from multiple magnetizations, Ludlow [7] describes the creation of MFL sizing models that take inputs from two magnetization directions. Danilov et al. [8] describe the application of multiple magnetization directions in a direct magnetic inversion solution. Their work highlights the potential geometry ambiguity inherent in the use of a single magnetization direction. It also demonstrates the strengths of a direct inversion solution using finite element methods to reveal the true geometry of metal loss. The primary drawback of the solution is the heavy computational load required to apply it, limiting the number of locations that can be assessed using the technique.

Failure Pressure Assessments

ASME B31G [9] describes common approaches to failure pressure assessment for corroded pipe. Early versions of the standard presented only what is now called the Original Method. Kiefner and Vieth [10] later described the Modified Method and the more sophisticated Effective Area Method (EAM), both of which are now incorporated into B31G. More recently, Kariyawasam et al. [11, 12] describe methods like Psqr, which extend EAM concepts to remove some excess conservatism under wide corrosion conditions. The EAM family of methods generally have less built-in model conservatism relative to the Original and Modified methods and require more accurate anomaly geometry for reliable application.

https://doi.org/10.52202/072781-0036

In the presence of complex, interacting corrosion, the selection of a failure pressure assessment method that is matched to the capabilities if the corrosion measurement system can be critical to obtaining reliable results. De Leon [13] describes the potential non-conservative assessment that can result when applying the EAM to metal loss anomalies that have been inadequately sized from axial MFL.

Methods

We present an ILI system and assessment approach that utilizes multiple magnetization directions simultaneously along with the EAM. The ILI data is gathered in a single inspection run that incorporates multiple magnetizers in the same tool train. The assessment approach is implemented in a production data analysis setting that scales to large quantities of corrosion anomalies.

Constructing and implementing a circumferential magnetizer has several challenges. The first is that, to generate a flux in the circumferential direction, the poles of at least two opposed magnets must be used. Figure 3(a) shows a circumferential magnetizer with four poles, two north and two south, arranged so that they are paired with opposite poles. Where the poles contact the pipe there is a blind spot where the field is entering into the pipe through the brushes. This is compensated for by having another circumferential magnetizing body oriented such that its inspectable area covers this blind spot.

Another alternative, though, is a magnetizer with a helical arrangement of magnets [14] that can provide complete circumferential inspection coverage in one body. As shown earlier in Figure 2, magnetizing the pipe at 45 degrees to the long axis of anomalies shows an MFL amplitude only slightly reduced from the full circumferential magnetization response. Thus, combining the axial MFL (AMFL) magnetizer and the SpirALL® MFL magnetizer (SMFL) in a single multiple dataset tool, shown in Figure 4, provides a complete inspection over all the range of geometries that can be inspected using the MFL technique with a single tool run.

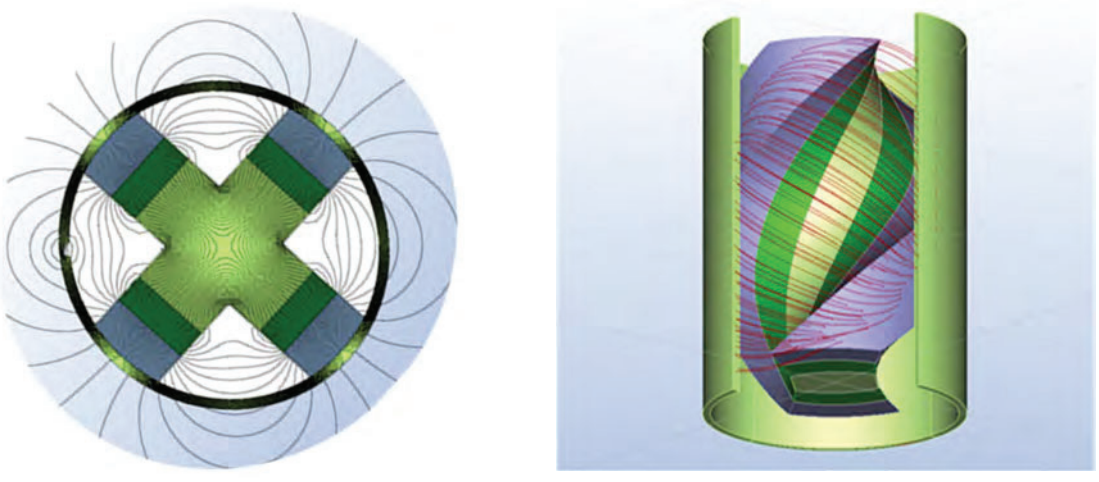

(a) Circumferential magnetizer (b) Spiral magnetizer

Figure 3. Schematic diagrams of non-axial magnetizers.

https://doi.org/10.52202/072781-0036

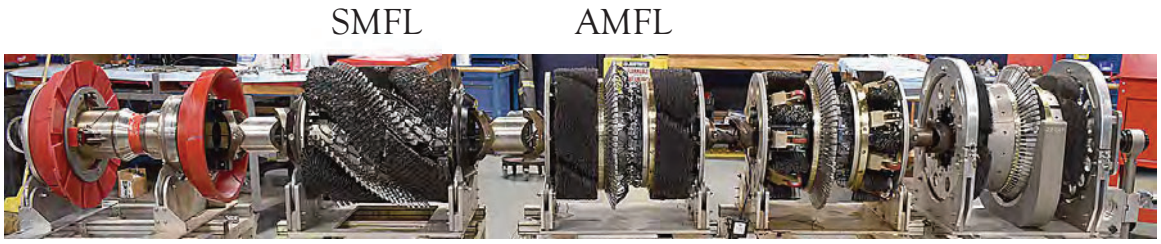

Figure 4. Multiple dataset ILI tool with both AMFL and SMFL magnetizers.

When used for metal loss sizing, AMFL and SMFL signal responses are complementary. AMFL has long been used for sizing of volumetric corrosion with enough circumferential extent to significantly disturb the field. Robust tools and mature sizing algorithms exist for AMFL. SMFL is better for both detecting and sizing narrow axial corrosion, long seam anomalies, selective seam weld corrosion, and crack-like anomalies that demonstrate some crack opening. In the case of tools with multiple magnetizations, robust sizing algorithms are available for both the AMFL and SMFL tool bodies. There are several steps to providing a joint analysis that is more accurate than the two components individually.

Mapping a pipe location between the two tool bodies must be accurate. Because of tool dynamics, it is not possible to use static tool geometry offsets alone to map pipe locations between tool bodies. An improved model of tool dynamics has improved body-to-body mapping. However, the location of an anomaly varies in the respective data sets because the magnetic response itself varies with irregular anomaly shapes. A computer vision model is employed to correlate AMFL and SMFL signature positions. The improvements to body-to-body mapping have other benefits for interactive threats, such as correlating corrosion to dent locations between the AMFL and caliper bodies.

Improved anomaly alignment capabilities have led to better automation. AMFL and SMFL signals are now associated automatically, allowing information from both technologies to be used in many more sizing calculations. The accuracy of the automation was measured on a set of 4,584 pits. The correlation between automatic signature matches and manual matches across the MFL technologies was found to be identical about 80% of the time.

With signatures aligned, the features used for sizing can be computed in both datasets. A decision-tree-based model is used to size corrosion in both AMFL and SMFL. Additionally, both AMFL and SMFL feature sets are combined to train a single model, called the Hybrid model, which improves sizing accuracy in most cases. The Hybrid model tends to improve accuracy by blending the AMFL and SMFL signal inputs in an optimal way, which is appropriate when both signals are present, distinct, and have similar magnitudes.

In many cases, the response of predominantly axial or circumferential anomalies can vary by several orders of magnitude between the AMFL and SMFL data. In this case, a machine learning technique called ensembling can determine how to optimally combine the results from multiple models. The Ensemble model uses predicted depths from the AMFL, SMFL, and Hybrid models together with other input features to compute an optimal depth call for each specific anomaly. The Ensemble model improves depth estimates uniformly but makes the largest improvement when the difference between AMFL and SMFL signals is large.

https://doi.org/10.52202/072781-0036

Figure 5 shows unity plots of the AMFL and the Ensemble models using 10 runs, or a total of 1,889 pits. Runs with many deep anomalies were chosen, as this is where the Ensemble model is expected to have the greatest impact. The Ensemble decreases the total squared error of the predicted depth by more than 20% relative to the AMFL model.

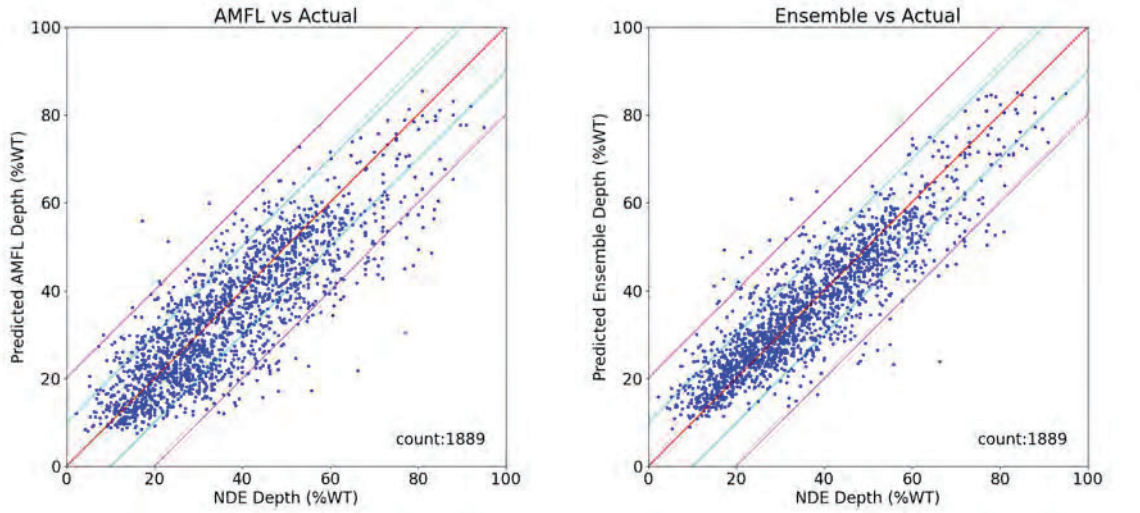

Figure 5. Model performance for the AMFL and Ensemble sizing models against a hold-out test set of depths obtained from field NDE. Units are fractional wall loss.

The application of multiple magnetizations provides broad detection coverage of both axial and circumferential anomaly presentations, and the accuracy of the resulting sizing models ensures that the use of EAM assessments will produce reliable failure pressure estimates. Clusters of anomalies are formed by interacting all marked metal loss, regardless of the dataset from which the anomaly originated—AMFL, SMFL or a combination of both.

Results

We present a brief case study on complex corrosion from a pipeline that exhibits both circumferential and axial corrosion patterns. Figure 6 shows one example of complex corrosion patterns resulting from spiral tape wrap coating failure that are elucidated by a combination of multiple magnetization directions.

In the analysis of this pipeline, approximately 37,000 individual metal loss anomalies were reported. Of those,

- 1,300 were sized using a combination of AMFL and SMFL signatures.
- 2,500 were sized using only SMFL signatures.
- The remaining were sized using only AMFL signatures.

https://doi.org/10.52202/072781-0036

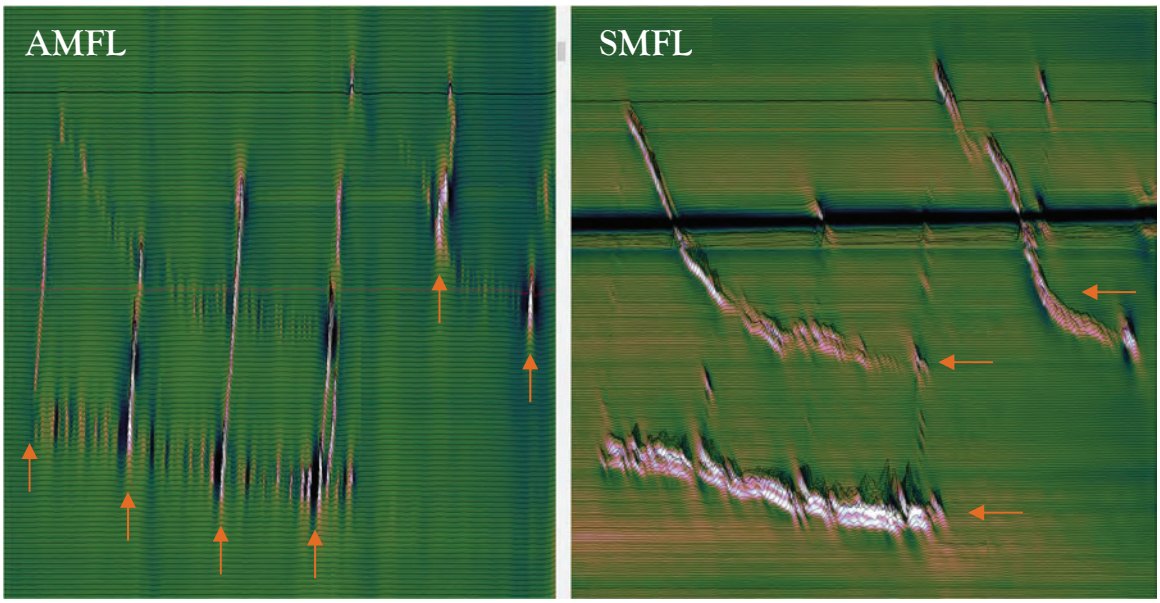

Figure 6. Corrosion patterns resulting from a tape wrap coating that is showing two failure patterns at the same location. Strong circumferential corrosion patterns appear at the overlap between wraps of the tape as visible in the AMFL data at left. Axial corrosion patterns appear where the coating is sagging and wrinkling as visible in the SMFL data at right. The dark horizontal band in the SMFL data is the long seam weld.

After sizing, all metal loss anomalies were clustered by applying a 6t (circumferential) × 6t (axial) interaction rule to all anomalies simultaneously, regardless of the signatures used to size them. Figure 7 displays a location where clusters were formed from a combination of metal loss sized from multiple magnetizations. The clusters contain anomalies sized from the various AMFL and SMFL signal contribution, including one axially oriented anomaly sized solely from the SMFL signal.

Performance of the ILI system against field nondestructive evaluation (NDE) techniques was evaluated on two criteria that align with common integrity management concerns.

1. Maximum metal loss depth (leak risk).

2. Estimated failure pressure ratio under the EAM (rupture risk).

The latter is a good indicator of how well each measurement technique captures anomaly length effects. In complex, interconnected corrosion clusters that can grow to be meters in length, individual anomaly boundaries that match against specific ILI metal loss call boxes are nearly impossible to establish in the field. The Original and Modified B31G Methods become very conservative under these conditions where the maximum observed anomaly depth is assumed to extend across the entire cluster length.

Field NDE techniques comprised a combination of laser scanning and pit gauge measurements. Figure 8 shows a unity plot of metal loss depth estimates from ILI and NDE. Figure 9 shows a unity plot of failure pressure ratio (FPR) with respect to maximum allowable operating pressure (MAOP) under the EAM as estimated from ILI and NDE results.

https://doi.org/10.52202/072781-0036

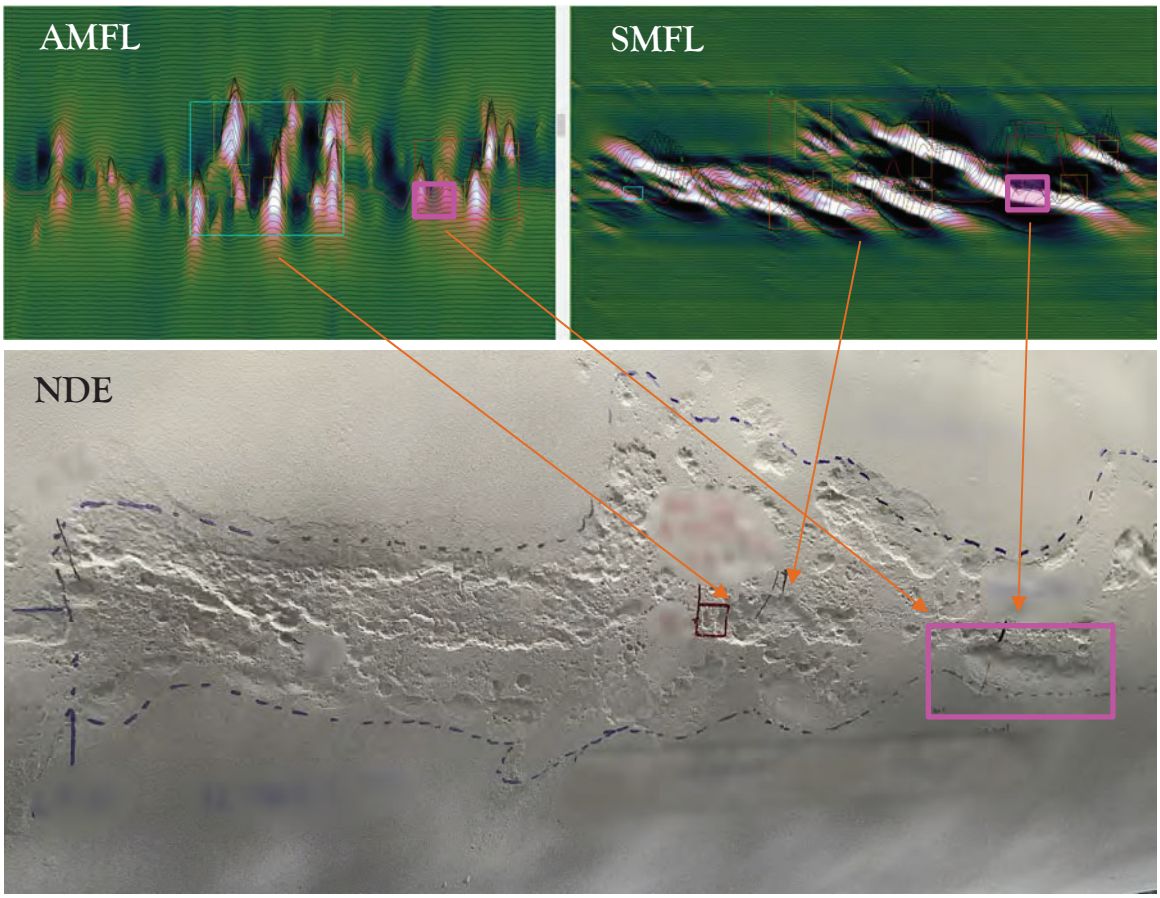

Figure 7. Complex corrosion with deep axially oriented anomaly (at right in NDE photo). The magenta boxes represent an anomaly sized from the SMFL data alone given very strong signal response, which provides the best estimate of maximum depth for the axially oriented anomaly. Maximum metal loss depth agreement between ILI and NDE at this anomaly was within 8% WT. FPR agreement between ILI and NDE at this anomaly was within 1%.

https://doi.org/10.52202/072781-0036

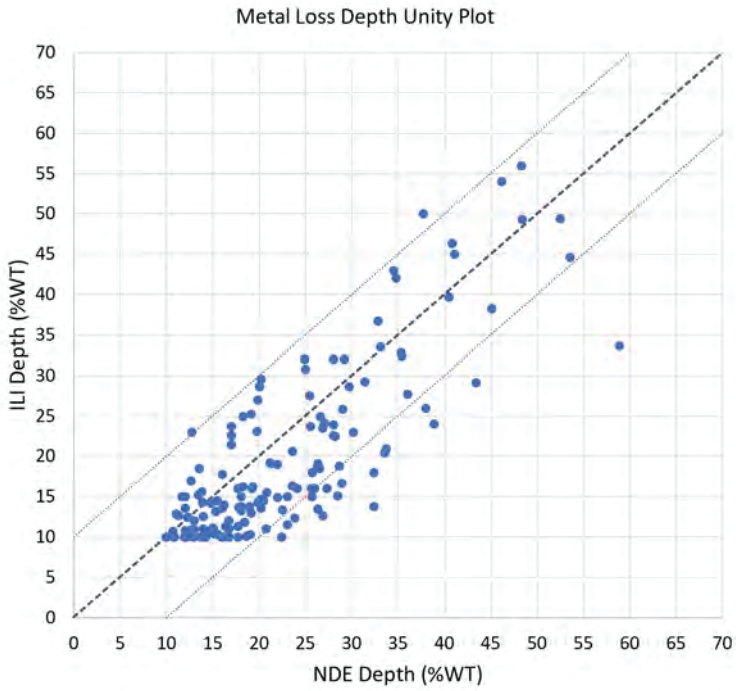

Figure 8. Unity plot of metal loss depths.

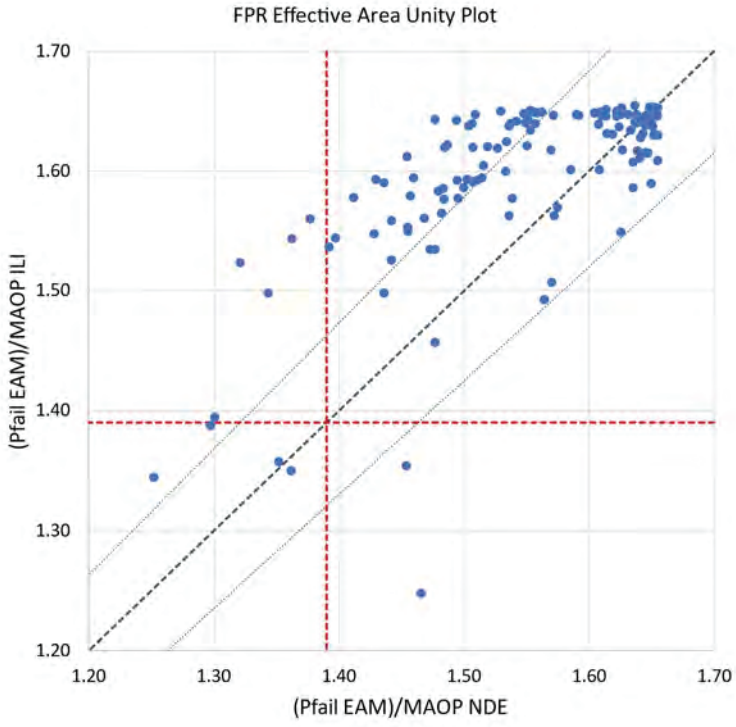

Figure 9. Unity plot of failure pressure ratios determined by the EAM. The error boundaries around unity represent ±5% difference between FPR from ILI and NDE. Red dashed lines represent typical repair thresholds for 1.39 factor of safety to MAOP.

https://doi.org/10.52202/072781-0036

Discussion

As Figure 8 suggests, agreement between maximum metal loss depth as estimated from ILI and NDE was excellent with a slight bias toward ILI undercall. Only one significant outlier was observed.

Differences in failure pressure ratio have two primary causes. Figure 10 shows two regions of the FPR unity plot where the largest deviations are observed.

1. In region 1, the ILI results predict an elevated failure pressure relative to NDE results due to cluster boundary differences. The NDE is forming longer clusters than the ILI due to shallow corrosion that interconnects regions of moderate corrosion depth. The shallow corrosion is unmarked in the ILI results because the metal loss in the area sizes below the reporting threshold of 10% WT. The additional connectedness of moderate corrosion patches in the NDE clusters results in a river bottom profile that produces a lower failure pressure estimate. In most cases in region 1, both the ILI and NDE results would recommend the same decision that a repair is not required. There are, however, five instances where NDE would recommend repair while ILI would not.
2. In region 2, the ILI results underpredict the failure pressure relative to NDE. These are both clusters where the ILI reports slightly deeper depths across the entire profile, resulting in a more conservative failure pressure than the NDE. In region 2, the ILI recommended repair where the NDE would not.

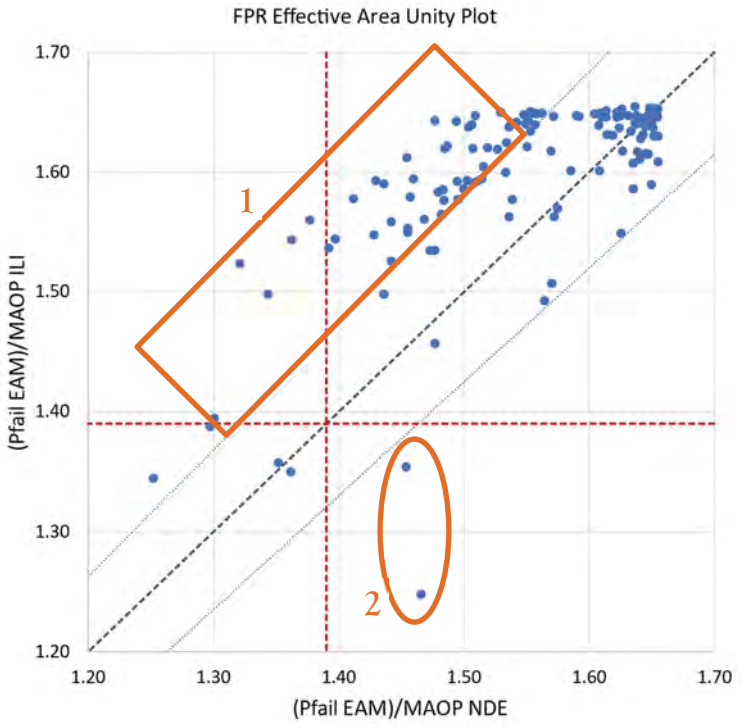

Figure 10. Two regions where meaningful failure pressure ratio differences are observed between ILI and NDE results.

Approaches to improving the agreement between NDE and ILI FPR under the EAM assessment have been published previously [15]. One approach is to apply a more conservative interaction rule to the

https://doi.org/10.52202/072781-0036

ILI results, such as 6t (circumferential) × 12t (axial), so that clusters grow longer in the axial direction to capture more regions of moderate metal loss that are separated only by very shallow corrosion that might go unmarked in the ILI results. Another approach is to lower the ILI depth reporting threshold for metal loss anomalies such that additional shallow corrosion is reported, and, in turn, clusters naturally grow longer to capture more regions of moderate corrosion that are connected only by shallow corrosion.

Referring again to Figure 10, although the FPRs obtained from NDE results are often more conservative than those obtained from ILI, this does not necessarily imply that the NDE FPRs are closer to ground truth. EAM assessments tend to overstate the potential effects of longitudinal anomaly interactions in a given river bottom profile as demonstrated in the historical RSTRENG validation work [16]. Stated another way, when anomaly interaction is known to be occurring, the EAM is an accurate estimator of failure pressure. However, the EAM algorithm itself is not necessarily an accurate predictor of which anomalies truly interact. As Figure 11 shows, where full-scale experimental results suggest that little anomaly interaction is occurring at anomaly spacings greater than 1.0 inch, the EAM algorithm overestimates the effects of anomaly proximity and returns a failure pressure prediction that is lower than the experimental results. Improved models for estimating the effects of anomaly interaction are under development [17], but, until those methods become widely available, failure predictions from the EAM applied to NDE laser scans serve as a more conservative proxy for ground truth.

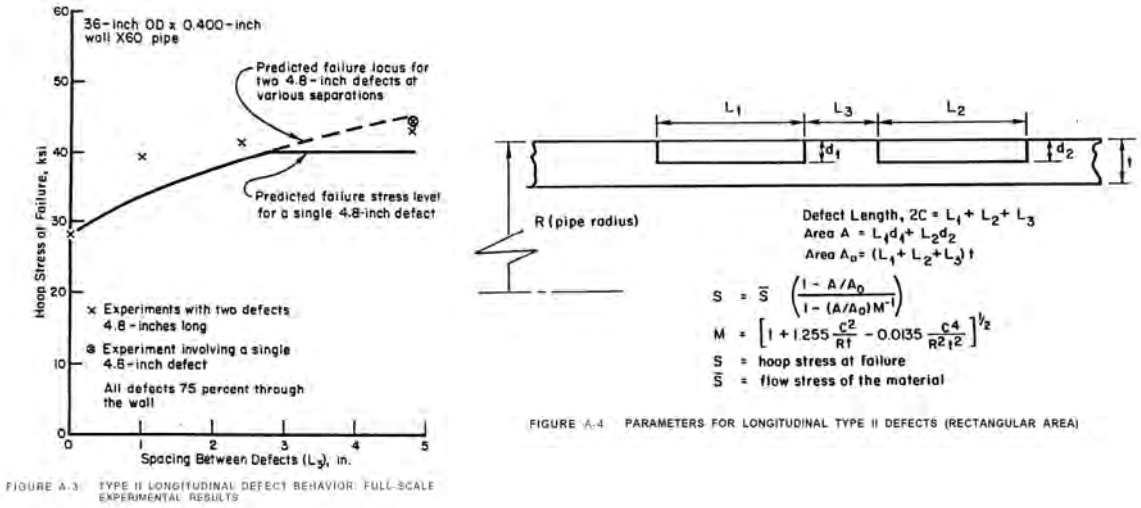

Figure 11. Influence of longitudinal spacing between anomalies on predicted failure pressure under the EAM, reproduced from the RSTRENG validation report [16]. The EAM generally overstates the effect of adjacent anomalies on predicted failure pressure where full scale tests would indicate less interaction of those adjacent anomalies.

Conclusions

The application of multiple magnetization directions to the detection and sizing of both circumferentially and axially oriented corrosion metal loss provides a suitable basis for applying the EAM for failure pressure assessment. The required datasets can be gathered in a single multiple-dataset ILI run. The analysis process can be applied in a production ILI data analysis setting and

https://doi.org/10.52202/072781-0036

scales to large quantities of corrosion anomalies. The agreement between NDE and ILI FPRs can be improved by clustering the ILI results in such a way that more regions of adjacent moderate corrosion are included into longer clusters.

Acknowledgements

We are deeply grateful to pipeline operators for granting permission to use the ILI and NDE data as part of the work presented in this paper.

References

[1] A. E. Crouch and R. C. Beaver, "Pipeline Inspection Apparatus for Detection of Longitudinal Defects". US Patent 3483466 A, 1969.

[2] J. B. Nestleroth, "Evaluation of Circumferential Magnetic Flux for In-Line Detection of Stress Corrosion Cracks and Selective Seam Weld Corrosion," PRCI, 1999.

[3] J. B. Nestleroth, "Circumferential MFL In-Line Inspection for Cracks in Pipelines," US Department of Energy, 2003.

[4] J. Simek, "Modeling and Results for Creating Oblique Fields in a Magnetic Flux Leakage Survey Tool," in *AIP Conference Proceedings 1211, 597 (2010).*

[5] J. B. Nestleroth, S. W. Rust, D. A. Burgoon and H. Haines, "Determining corrosion defect geometry from magnetic flux leakage pig data," in *NACE Corrosion Conference 1996*, Houston, 1996.

[6] H. Haines, P. Porter and L. Barkdull, "Advanced Magnetic Flux Leakage Signal Analysis for Detection and Sizing of Pipeline Corrosion," in *2nd International Pipeline Week*, Houston, 1998.

[7] J. Ludlow, "Enhancing Metal Loss Sizing Using Multiple Data Sets," in *26th International Pipeline Pigging and Integrity Management Conference (PPIM 2014)*, Houston, 2014.

[8] A. Danilov, J. Palmer, A. Schartner and V. Tse, "Computing 3D Metal Loss from MFL ILI Data for Reliable Safe Pressure Prediction, IBP1018_19," in *Proceedings of the Rio Pipeline Conference 2019*, Rio de Janeiro, 2019.

[9] American Society of Mechanical Engineers, "B31G-2023 Manual for Determining the Remaining Strength of Corroded Pipelines," ASME, New York, 2023.

[10] J. F. Kiefner and P. H. Vieth, "A modified criterion for evaluating the remaining strength of corroded pipe," Pipeline Research Council International, 1989, Catalog No. L51688Be.

[11] S. Kariyawasam, S. Zhang, J. Yan, T. Huang, M. Al-Amin and E. Gamboa, "Plausible Profiles (Psqr) Model for Corrosion Assessment: Report to PRCI Corrosion Technical Committee," TC Energy, June 7, 2019.

[12] S. Zhang, J. Yan, S. Kariyawasam, T. Huang and M. Al-Amin, "Plausible Profile (Psqr) Corrosion Assessment Model: Refinement, Validation and Operationalization," in *2020 13th International Pipeline Conference*, Calgary, CA, 2021.

[13] C. De Leon, "Know when using MFL for Effective Area is wrong!," in *35th International Pipeline Pigging and Integrity Management Conference (PPIM 2023)*, Houston, 2023.

[14] J. S. Simek, J. Ludlow and P. Tisovec, "Oblique Field Magnetic flux Leakage Inline Survey Tool," in *Proceedings of IPC2004*, Calgary, Alberta, Canada, 2010.

https://doi.org/10.52202/072781-0036

[15] J. Ludlow and J. Hardy, "Minimizing the Error in Corrosion Growth Rate Estimation from Box-to-Signal Matching," in *35th International Pipeline Pigging and Integrity Management Conference (PPIM 2023)*, Houston, 2023.

[16] J. F. Kiefner, P. H. Vieth and I. Roytman, "Continued Validation of RSTRENG, L51749e," Pipeline Research Council International, 1996.

[17] Pipeline Research Council International, "EC-2-10: Deliver Comprehensive Metal-Loss Assessment Criterion," [Online]. Available: https://www.prci.org/Research/Corrosion/CORRProjects/EC-2-10.aspx. [Accessed 19 December 2023].

https://doi.org/10.52202/072781-0036